

# Nonsingular bounce revisited

F.R. Klinkhamer\*

*Institute for Theoretical Physics,  
Karlsruhe Institute of Technology (KIT),  
76128 Karlsruhe, Germany*

## Abstract

The big bang singularity of the Friedmann solution for an expanding universe can be regularized by the introduction of a nonzero length scale  $b$ . The result is a nonsingular bounce of the cosmic scale factor  $a(T)$  with a contracting pre-bounce phase and an expanding post-bounce phase. The corresponding maximum values of the curvature and the energy density occur at the moment of the bounce and are proportional to powers of  $1/b$ . This article presents a detailed calculation of the dynamics of such a nonsingular bounce.

PACS numbers: 04.20.Cv, 98.80.Bp, 98.80.Jk

Keywords: general relativity, big bang theory, mathematical and relativistic aspects of cosmology

---

\* frans.klinkhamer@kit.edu

## I. INTRODUCTION

The big bang singularity of the Friedmann solution [1, 2] for an expanding universe (assumed to be homogeneous and isotropic) can be regularized [3] by the introduction of a nonzero length scale  $b$  and a 3-dimensional submanifold of spacetime with a vanishing determinant of the metric. The original big bang singularity [at cosmic time coordinate  $t = t_{\text{bb}}$  with vanishing cosmic scale factor  $a(t_{\text{bb}}) = 0$ ] is replaced by a 3-dimensional “defect” of spacetime [the defect occurs at cosmic time coordinate  $T = T_B$  and has a cosmic scale factor  $a(T_B) \neq 0$ , for a new coordinate  $T$  which will be defined later]. Two follow-up papers [4, 5] discuss certain aspects of the resulting nonsingular bouncing cosmology. (See, e.g., Ref. [6] for a review of the basic ideas of nonsingular bouncing cosmology and an extensive list of references.)

The calculations of the follow-up papers [4, 5] used an auxiliary cosmic time coordinate  $\tau = \tau(T)$ , for which the reduced field equations are nonsingular and, therefore, directly accessible to numerical analysis. These reduced field equations are, in fact, ordinary differential equations (ODEs) and we call them the  $\tau$ -ODEs. But the auxiliary coordinate  $\tau$  differs essentially from the cosmic time coordinate  $T$  which enters the metric. The corresponding reduced field equations in terms of  $T$  are singular ODEs and precisely the singularities in these  $T$ -ODEs force the solution  $a(T)$  to be nonsingular, with a nonzero cosmic scale factor  $a(T_B) \neq 0$  at the moment of the cosmic bounce,  $T = T_B$ .

The goal of the present article is to carefully study these singular  $T$ -ODEs, in order to understand the dynamics of the time-symmetric nonsingular bounce. The outline is as follows. In Sec. II, we recall the *Ansatz* for the metric from Ref. [3], and discuss an advantage and a disadvantage of this *Ansatz*. In Sec. III, we present a new *Ansatz* for the metric. In Sec. IV, we obtain analytic and numerical results for this new metric, where the main focus is on establishing the smooth behavior of physical quantities at the bounce. In Sec. V, we address the subtle issue of boundary conditions.

## II. PREVIOUS METRIC ANSATZ (MODEL 1)

For a modified spatially flat Friedmann–Lemaître–Robertson–Walker (FLRW) universe with cosmic time coordinate  $T$  and comoving spatial Cartesian coordinates  $\{x^1, x^2, x^3\}$ , the

simplest *Ansatz* for a degenerate metric is given by [3]

$$ds^2 \Big|^{(\text{model 1})} \equiv g_{\mu\nu}(x) dx^\mu dx^\nu \Big|^{(\text{model 1})} = -\frac{T^2}{T^2 + b^2} dT^2 + \tilde{a}^2(T) \delta_{kl} dx^k dx^l, \quad (2.1a)$$

$$b > 0, \quad (2.1b)$$

$$T \in (-\infty, \infty), \quad x^k \in (-\infty, \infty), \quad (2.1c)$$

where  $b$  corresponds to the length scale of a spacetime defect (cf. Refs. [7, 8] and references therein). For definiteness, we call this previous metric (2.1a) the “model-1” metric. The metric from (2.1a) is degenerate, having  $\det g_{\mu\nu} = 0$  at  $T = 0$ .

We assume that the matter content is described by a homogeneous perfect fluid with energy density  $\rho_M(T)$  and pressure  $P_M(T)$ . From the Einstein gravitational field equation [2] and the metric (2.1a), we then obtain the dynamic equations for the variables  $\tilde{a}(T)$  and  $\rho_M(T)$ . These equations are the energy-conservation equation of the matter, the equation of state relating  $P_M(T)$  to  $\rho_M(T)$ , the modified first-order spatially flat Friedmann equation, and the modified second-order spatially flat Friedmann equation:

$$\rho'_M + 3 \frac{\tilde{a}'}{\tilde{a}} [\rho_M + P_M] = 0, \quad (2.2a)$$

$$P_M = P_M(\rho_M), \quad (2.2b)$$

$$\left[1 + \frac{b^2}{T^2}\right] \left(\frac{\tilde{a}'}{\tilde{a}}\right)^2 = \frac{8\pi G_N}{3} \rho_M, \quad (2.2c)$$

$$\left[1 + \frac{b^2}{T^2}\right] \left(\frac{\tilde{a}''}{\tilde{a}} + \frac{1}{2} \left(\frac{\tilde{a}'}{\tilde{a}}\right)^2\right) - \frac{b^2}{T^3} \frac{\tilde{a}'}{\tilde{a}} = -4\pi G_N P_M, \quad (2.2d)$$

where the prime stands for differentiation with respect to  $T$ . The ODEs (2.2c) and (2.2d) reproduce, in the limit  $b \rightarrow 0$ , the standard Friedmann equations [2]. Remark also that, if  $\tilde{a}'(T)$  were to vanish at a cosmic time  $T = T_{\text{stop}} \neq 0$ , this would require a vanishing energy density,  $\rho_M(T_{\text{stop}}) = 0$ , according to (2.2c).

The advantage of the metric (2.1a) is that it takes the standard FLRW form,

$$ds^2 \Big|^{(\text{model 1, } \tau\text{-coord.})} = -d\tau^2 + \hat{a}^2(\tau) \delta_{kl} dx^k dx^l, \quad (2.3)$$

if we replace the coordinate  $T$  by the coordinate  $\tau$ , which is defined as follows:

$$\tau(T) = \begin{cases} +\sqrt{b^2 + T^2}, & \text{for } T \geq 0, \\ -\sqrt{b^2 + T^2}, & \text{for } T \leq 0, \end{cases} \quad (2.4)$$

where  $\tau = -b$  and  $\tau = b$  correspond to the single point  $T = 0$  on the cosmic time axis. The coordinate transformation (2.4) is non-invertible (two different  $\tau$  values for  $T = 0$ ) and is not a diffeomorphism. This implies that the differential structure of the spacetime manifold with metric (2.1a) differs from the differential structure of the spacetime manifold with metric (2.3); see Ref. [8] for an extensive discussion. For practical calculations [4, 5], the metric (2.3) is to be preferred, as the corresponding  $\tau$ -ODEs are nonsingular.

But, with the different differential structure from (2.1a) and (2.3), the actual study of the bounce at  $T = 0$  requires the  $T$ -ODEs. The disadvantage of the metric *Ansatz* (2.1a), then, is that it explicitly depends on the coordinate  $T$ , as do the corresponding ODEs (2.2c) and (2.2d). It would be preferable to have a metric that depends only on the scale factor and its derivatives.

### III. NEW METRIC ANSATZ (MODEL 2)

We now present a new metric *Ansatz* for a modified spatially flat FLRW universe, with the metric depending only on the scale factor and its derivatives. For definiteness, we call this new metric the “model-2” metric. Specifically, the new metric reads

$$ds^2 \Big|^{(\text{model 2})} = -\frac{[a(T) - a_B]^2}{[a(T) - a_B]^2 + b^2 [a'(T)/2]^2} dT^2 + a^2(T) \delta_{kl} dx^k dx^l, \quad (3.1a)$$

$$b > 0, \quad (3.1b)$$

$$a(T) > 0, \quad (3.1c)$$

$$a'(T_B) = 0, \quad (3.1d)$$

$$a(T_B) \equiv a_B > 0, \quad (3.1e)$$

$$T \in (-\infty, \infty), \quad x^k \in (-\infty, \infty), \quad (3.1f)$$

where the prime, again, stands for differentiation with respect to  $T$ . The moment of the bounce,  $T = T_B$ , is determined by (3.1d) and the corresponding value of the scale factor is denoted  $a_B$ , as stated in (3.1e).

We observe that close to the bounce, with  $a(T) \sim a_B + c_2 T^2$  for  $T_B = 0$  and a constant  $c_2$ , the  $g_{00}$  component from (3.1a) reduces to the expression  $-T^4/(T^4 + b^2 T^2)$ , which has essentially the same structure as the  $g_{00}$  component of the model-1 metric (2.1a). In principle,

it is also possible to consider a metric *Ansatz* without explicit mention of  $a_B$  (an example would be  $g_{00} = -(a')^2/[(a')^2 + b^2(a'')^2]$ ), but the *Ansatz* (3.1a) suffices for the purpose of studying the bounce dynamics.

Assume, again, that the matter content is given by a homogeneous perfect fluid. From the Einstein gravitational field equation [2] and the metric (3.1a), we obtain the dynamic equations for the variables  $a(T)$  and  $\rho_M(T)$ . These equations are the energy-conservation equation of the matter, the equation of state of the matter, the modified first-order spatially flat Friedmann equation, and the modified second-order spatially flat Friedmann equation:

$$\rho'_M + 3 \frac{a'}{a} [\rho_M + P_M] = 0, \quad (3.2a)$$

$$P_M = P_M(\rho_M), \quad (3.2b)$$

$$\left(\frac{a'}{a}\right)^2 + \frac{b^2 a'^4}{a^2 [a - a_B]^2} = \frac{8\pi G_N}{3} \rho_M, \quad (3.2c)$$

$$\left[1 + \frac{1}{2} \frac{b^2 [a']^2}{[a - a_B]^2}\right] \frac{a''}{a} + \frac{1}{2} \left(\frac{a'}{a}\right)^2 + \frac{1}{8} b^2 \frac{a^2 [a + a_B]}{[a - a_B]^3} \left(\frac{a'}{a}\right)^4 = -4\pi G_N P_M. \quad (3.2d)$$

We have the following remarks:

1. The ODEs (3.2c) and (3.2d) reproduce, in the limit  $b \rightarrow 0$ , the standard Friedmann equations [2].
2. Precisely the  $b^2$  terms of the ODEs (3.2c) and (3.2d) have various powers of the factor  $a'(T)/[a(T) - a_B]$  which is singular at  $T = T_B$ .
3. It is possible to verify that the second-order ODE (3.2d) is consistent with the first-order ODEs (3.2a) and (3.2c); cf. the discussion in Sec. 15.1 of Ref. [2] for the case of the standard Friedmann equations.
4. The ODEs (3.2a), (3.2c), and (3.2d) are invariant under the rescaling  $a(T) \rightarrow \zeta a(T)$ , which implies  $a_B \rightarrow \zeta a_B$  from (3.1e), and also under time reversal  $(T - T_B) \rightarrow -(T - T_B)$ .

From now on, we assume that the matter content is described by a homogeneous perfect fluid with a constant equation-of-state parameter,

$$W_M(T) \equiv P_M(T)/\rho_M(T) = w_M = \text{constant}. \quad (3.3)$$

Furthermore, we use reduced-Planckian units, with

$$8\pi G_N = c = \hbar = 1, \quad (3.4)$$

and take the following model parameters:

$$b = 1, \quad (3.5a)$$

$$w_M = 1, \quad (3.5b)$$

where this particular choice for  $w_M$  aims to avoid possible instabilities in the pre-bounce phase [6]. In order to compare with previous results, we choose

$$T_B = 0, \quad (3.5c)$$

$$a_B = 1, \quad (3.5d)$$

but the value of  $T_B$  can be arbitrarily shifted and the value of  $a_B$  can be arbitrarily rescaled.

## IV. BOUNCE SOLUTION OF MODEL-2 ODES

### A. Analytic results

We start from the well-known analytic solution [2] of (3.2a) for the case of a constant equation-of-state parameter  $w_M$  as defined by (3.3):

$$\rho_M(a) = r_0 a^{-3[1+w_M]}, \quad (4.1a)$$

$$r_0 > 0, \quad (4.1b)$$

where  $a(T)$  is normalized by (3.5c) and (3.5d). Near  $T = T_B = 0$ , the resulting ODEs (3.2c) and (3.2d) are approximately solved by a truncated power series,

$$a(T) = 1 + \sum_{n=1}^N a_{2n} (T/b)^{2n}. \quad (4.2)$$

With  $N = 4$ , we obtain the following coefficients (taking the positive root for  $a_2$ ):

$$a_2 = \frac{1}{2\sqrt{3}} b \sqrt{r_0}, \quad (4.3a)$$

$$a_4 = -\frac{1}{72\sqrt{3}} \left( 6b\sqrt{r_0} + \sqrt{3}b^2 r_0 [1 + 3w_M] \right), \quad (4.3b)$$

$$a_6 = \frac{1}{25920} b \sqrt{r_0} \left( 156\sqrt{3} + 48b\sqrt{r_0} [1 + 3w_M] + \sqrt{3}b^2 r_0 [31 + 132w_M + 117w_M^2] \right), \quad (4.3c)$$

$$a_8 = -\frac{1}{362880\sqrt{3}} b \sqrt{r_0} \left( 1044 - 72\sqrt{3}b\sqrt{r_0} [1 + 3w_M] + 9b^2 r_0 [29 + 120w_M + 99w_M^2] \right. \\ \left. + 2\sqrt{3}b^3 r_0^{3/2} [77 + 405w_M + 621w_M^2 + 297w_M^3] \right), \quad (4.3d)$$

where  $r_0$  in the expressions (4.3) really corresponds to  $8\pi G_N r_0$  with mass dimension 2. For  $b = 1$ ,  $w_M = 1$ , and  $r_0 = 1/3$ , we have

$$\{a_2, a_4, a_6, a_8\} \Big|_{b=1, w_M=1, r_0=1/3} \approx \{0.166667, -0.0462963, 0.0120885, -0.0022352\}, \quad (4.4)$$

which suggests an alternating series.

Returning to the  $a_2$  solution (4.3a), the relevant equation is the series expansion of the modified first-order spatially flat Friedmann equation (3.2c), which reads

$$0 = 4(a_2)^2/b^2 - r_0/3 + O(T^2), \quad (4.5)$$

for  $8\pi G_N = 1$ . As said, we have chosen the positive root for  $a_2$  and we postpone further discussion to Sec. V.

The Ricci curvature scalar  $R(x) \equiv g^{\nu\sigma}(x) g^{\mu\rho}(x) R_{\mu\nu\rho\sigma}(x)$  and the Kretschmann curvature scalar  $K(x) \equiv R^{\mu\nu\rho\sigma}(x) R_{\mu\nu\rho\sigma}(x)$  are readily evaluated for the metric (3.1a). The resulting expressions are functionals of the *Ansatz* function  $a(T)$ . Inserting the truncated series (4.2), we obtain

$$R(T) = \frac{1}{b^2} \sum_{n=0}^{N'} R_{2n} (T/b)^{2n}, \quad (4.6)$$

$$K(T) = \frac{1}{b^4} \sum_{n=0}^{N''} K_{2n} (T/b)^{2n}. \quad (4.7)$$

With the  $a$ -coefficients from (4.3) for  $2N = 8$ , we have

$$R_0 = b^2 r_0 (1 - 3 w_M) , \quad (4.8a)$$

$$R_2 = -\frac{1}{2} \sqrt{3} b^3 r_0^{3/2} (1 - 2 w_M - 3 w_M^2) , \quad (4.8b)$$

$$R_4 = \frac{1}{24} b^3 r_0^{3/2} (1 - 2 w_M - 3 w_M^2) \left( 2 \sqrt{3} + b \sqrt{r_0} [13 + 12 w_M] \right) , \quad (4.8c)$$

and

$$K_0 = \frac{1}{3} b^4 r_0^2 (5 + 6 w_M + 9 w_M^2) , \quad (4.9a)$$

$$K_2 = -\frac{1}{\sqrt{3}} b^5 r_0^{5/2} (5 + 11 w_M + 15 w_M^2 + 9 w_M^3) , \quad (4.9b)$$

$$K_4 = \frac{1}{36} b^5 r_0^{5/2} (5 + 11 w_M + 15 w_M^2 + 9 w_M^3) \left( 2 \sqrt{3} + b \sqrt{r_0} [22 + 21 w_M] \right) . \quad (4.9c)$$

The perturbative results (4.8) for  $2N' = 4$  suggest that  $R(T) = 0$  for the case of relativistic matter with  $w_M = 1/3$ , just as for the standard FLRW universe [2]. The numerical values of the coefficients (4.8) and (4.9) for  $b = 1$ ,  $w_M = 1$ , and  $r_0 = 1/3$  are

$$\{R_0, R_2, R_4\} \Big|_{b=1, w_M=1, r_0=1/3} \approx \{ -0.666667, 0.666667, -0.574074 \} , \quad (4.10a)$$

$$\{K_0, K_2, K_4\} \Big|_{b=1, w_M=1, r_0=1/3} \approx \{ 0.740741, -1.48148, 2.01646 \} . \quad (4.10b)$$

For completeness, we also give the asymptotic solution for  $T^2 \rightarrow \infty$ ,

$$a_{\text{asyp}}(T) \sim a_\infty (T^2)^{p/2} , \quad (4.11a)$$

$$\rho_{M \text{ asyp}}(T) \sim r_\infty [a_{\text{asyp}}(T)]^{-3[1+w_M]} , \quad (4.11b)$$

$$a_\infty = \left( \frac{r_\infty}{3 p^2} \right)^{p/2} , \quad (4.11c)$$

$$p = \frac{2}{3} \frac{1}{1 + w_M} , \quad (4.11d)$$

where the constant  $r_\infty$  depends indirectly on the constant  $r_0$  from (4.1).

In closing, we remark that we have seen that the solution  $\bar{a}(T)$  of the ODEs (3.2) can be expanded perturbatively around  $T = T_B = 0$ . The obtained Taylor series is characterized by the numerical value of  $r_0$ , as the values of  $T_B$  and  $a_B$  can be changed arbitrarily (here, they are taken as  $T_B = 0$  and  $a_B = 1$ ). The asymptotic solution for  $a(T)$  has also been seen to depend indirectly on  $r_0$ .



## B. Numerical results

We are able to obtain a close approximation of the exact solution  $\bar{a}(T)$  of the ODEs (3.2), for a constant equation-of-state parameter  $w_M$  from (3.3), by using the truncated power series (4.2) for a small enough interval around  $T = T_B = 0$  and by solving the ODEs numerically for  $T$  values outside this interval. Specifically, we take for the power-series interval  $[-\Delta T, \Delta T]$  and truncate the series (4.2) at  $2N = 8$ . In principle, we must take  $\Delta T \rightarrow 0$  and  $N \rightarrow \infty$ . We leave a detailed study of the numerical convergence properties to the future, as well as a determination (if at all possible) of the radius of convergence of the series corresponding to (4.2). For the moment, we have just compared the results for different values of  $\Delta T$  (specifically, 1/100 or 1/10) and different values of  $N$  (specifically, 4 or 8), and find the results to be reasonably stable.

For the numerical solution of the ODEs (3.2), we can focus on the modified first-order Friedmann ODE (3.2c). The reason is that (3.2a) already has the analytic solution (4.1a) and that, as mentioned before, the second-order Friedmann ODE (3.2d) follows from the first-order ODEs (3.2a) and (3.2c).

As to the numerical solution of the ODE (3.2c), there are two subtleties. This paragraph can, however, be skipped in a first reading. The first subtlety is that the ODE (3.2c) is not directly accessible to numerical analysis, as the equation is quadratic in  $[a']^2 \equiv S$ . But we can obtain analytically the positive root of this quadratic equation for  $S$ . Then, we take the square root of  $S$ , with a minus sign of the resulting expression for  $a'$  in the pre-bounce phase and a plus sign in the post-bounce phase. The second subtlety is that we do not numerically solve the obtained ODEs which are linear in  $a'$  (with different signs for the pre- and post-bounce phases), but rather numerically solve the first derivative of these first-order ODEs. In this way, we obtain a numerical solution with a reasonably accurate value of  $a''(T)$  at  $T = \pm\Delta T$ . In fact, we can check for the accuracy of the obtained numerical solution  $a_{\text{num}}(T)$  by evaluating the residue of the second-order ODE (3.2d).

Analytic and numerical results for  $b = 1$ ,  $w_M = 1$ , and  $r_0 = 1/3$  are given in Fig. 1. As noted in the last paragraph of Sec. IV A, the solution is characterized by the numerical value of  $r_0$ , for fixed values of the model parameters  $b$  and  $w_M$ . We give the results for a smaller numerical value of  $r_0$  in Fig. 2, where the  $\rho_M$  peak is lower and somewhat broader than the one in Fig. 1. The corresponding plots for the Ricci curvature scalar  $R(T)$  and the

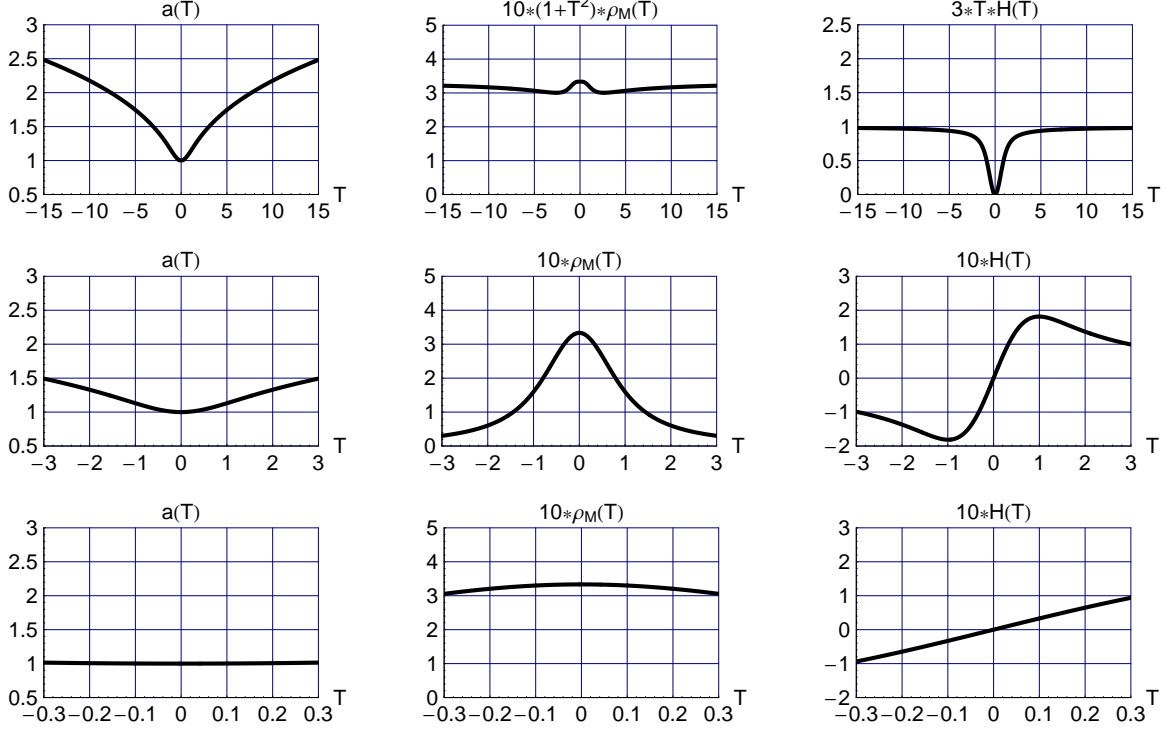


FIG. 1. Solution of the ODEs (3.2a) and (3.2c) for a constant equation-of-state parameter  $w_M$  from (3.3) and reduced-Planckian units (3.4). The model parameters are  $b = 1$  and  $w_M = 1$ . The boundary conditions at  $T = T_B = 0$  are  $a(0) \equiv a_B = 1$  and  $\rho_M(0) = r_0$  for  $r_0 = 1/3$ . The analytic solution is shown over  $T \in [-\Delta T, \Delta T]$  and the numerical solution over  $T \in [-T_{\max}, -\Delta T] \cup [\Delta T, T_{\max}]$ , with  $\Delta T = 1/10$  and  $T_{\max} = 15$ . Specifically, the analytic solution for  $a(T)$  is given by (4.2) and (4.4) for  $N = 4$ , while the analytic solution for  $\rho_M(T)$  follows from (4.1). The numerical solution is obtained from the ODEs (3.2a) and (3.2c) with boundary conditions at  $T = \pm \Delta T$  from the analytic solution. Shown, on the top row, are the dynamic functions  $a(T)$  and  $\rho_M(T)$ , together with the corresponding Hubble parameter  $H(T) \equiv [da(T)/dT]/a(T)$ . The middle and bottom rows zoom in on the bounce at  $T = T_B = 0$ . In the middle panel of the top row,  $10\rho_M(T)$  is scaled by a further factor  $(1 + T^2)$ , in order to display the asymptotic behavior  $\rho_M(T) \propto 1/T^2$ . Similarly, in the right panel of the top row,  $H(T)$  is scaled by a factor  $3T$ , in order to display the asymptotic behavior  $H(T) \sim (1/3)T^{-1}$ .

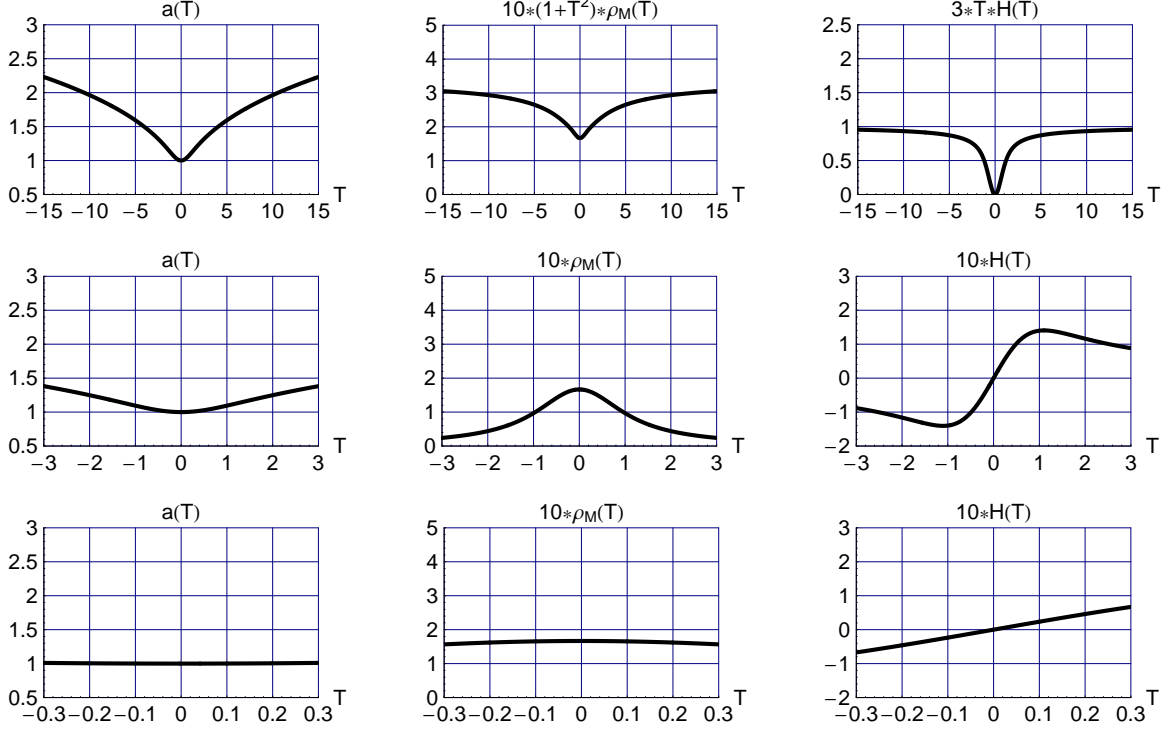


FIG. 2. Same as Fig. 1, but now with boundary condition  $\rho_M(0) = r_0 = 1/6$ .

Kretschmann curvature scalar  $K(T)$  are given in Figs. 3 and 4.

The top-right panels in Figs. 1 and 2 show the asymptotic behavior  $H(T) \sim (1/3)T^{-1}$ , which results from the asymptotic behavior  $a(T) \propto (T^2)^{1/6}$ . The bottom rows in Figs. 1 and 2 illustrate the smooth behavior at the bounce  $T = T_B = 0$ . The smooth behavior at the bounce is also evident from the perturbative result (4.6) for the Ricci curvature scalar  $R(T)$  and the perturbative result (4.7) for the Kretschmann curvature scalar  $K(T)$ , as shown on the bottom rows of Figs. 3 and 4.

## V. DISCUSSION

We have presented, in Sec. III, a new metric *Ansatz* for a modified spatially flat FLRW universe. For the case of a constant equation-of-state parameter  $w_M = 1$ , we have obtained, in Sec. IV, analytic results in a small interval around the cosmic time  $T = T_B = 0$  of the time-symmetric bounce, together with numerical results for larger values of  $|T|$ . The solution  $\bar{a}(T)$  is regular at  $T = T_B$  and appears to be well-behaved for finite values of  $|T|$ .

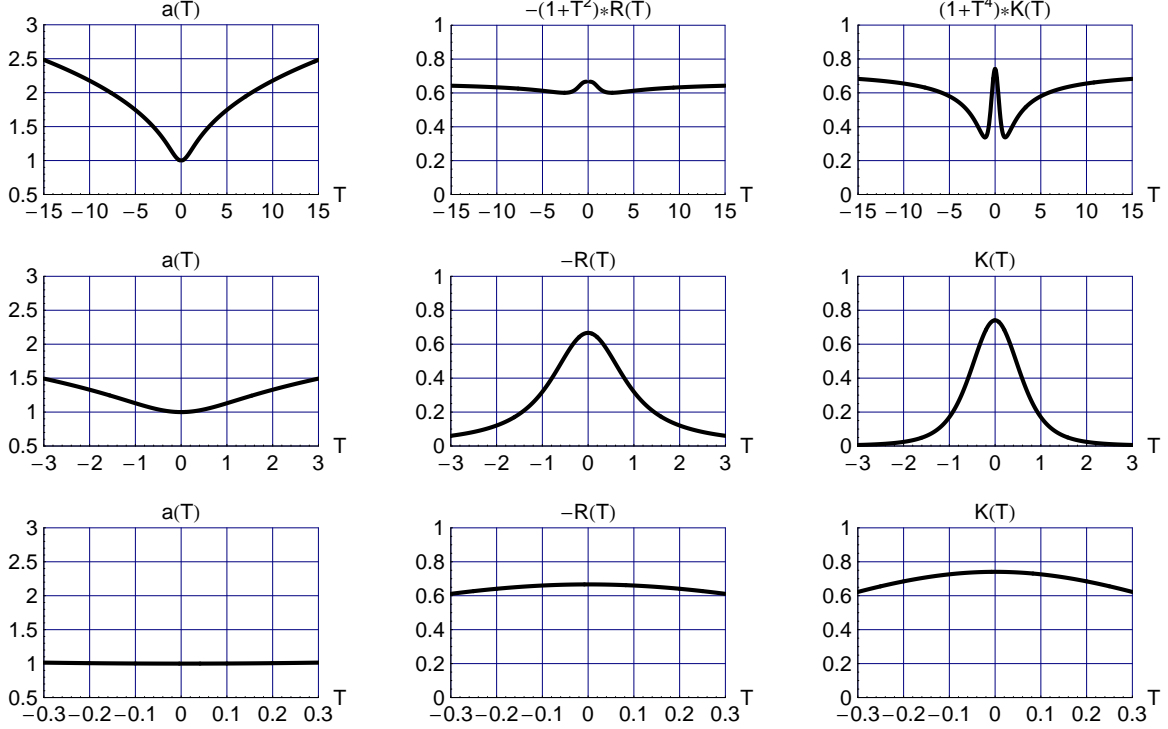


FIG. 3. Ricci curvature scalar  $R(T)$  and Kretschmann curvature scalar  $K(T)$  for the solution  $a(T)$  of Fig. 1. In the middle panel of the top row,  $-R(T)$  is scaled by a factor  $(1 + T^2)$ , in order to display the asymptotic behavior  $-R(T) \propto 1/T^2$ . Similarly, in the right panel of the top row,  $K(T)$  is scaled by a factor  $(1 + T^4)$ , in order to display the asymptotic behavior  $K(T) \propto 1/T^4$ .

The solution  $\bar{a}(T)$  is characterized by the maximum energy density  $\rho_M(T)$  of the matter, which occurs at  $T = T_B$ . The dimensionless quantity for this maximum energy density is denoted  $r_0$ , and the behavior of the analytic and numeric solutions in Figs. 1 and 2 is controlled by  $r_0$  only, for fixed model parameters  $b$  and  $w_M$ .

As mentioned in Sec. IV A, the behavior of the  $a(T)$  series solution near  $T = T_B = 0$  has been chosen to be convex ( $a_2 > 0$  with  $a_B = 1$ ). In principle, it is also possible to have an  $a(T)$  solution near  $T = T_B$  that is concave ( $a_2 < 0$  with  $a_B = 1$ ), so that there will be cosmic times  $T_{\pm} = T_B \pm \Delta T_{\text{bb}}$  with a vanishing scale factor,  $a(T_{\pm}) = 0$ . The different bounces, convex and concave at  $T = T_B$ , result from different initial conditions at  $T_{\text{start}} < T_B$ . Taking  $a(T_{\text{start}}) > a_B$  and  $a'(T_{\text{start}}) < 0$  gives a convex bounce, with a contracting phase for  $T \in [T_{\text{start}}, T_B]$  and an expanding phase for  $T \in (T_B, \infty)$ . An explicit calculation with initial conditions is presented in App. A.

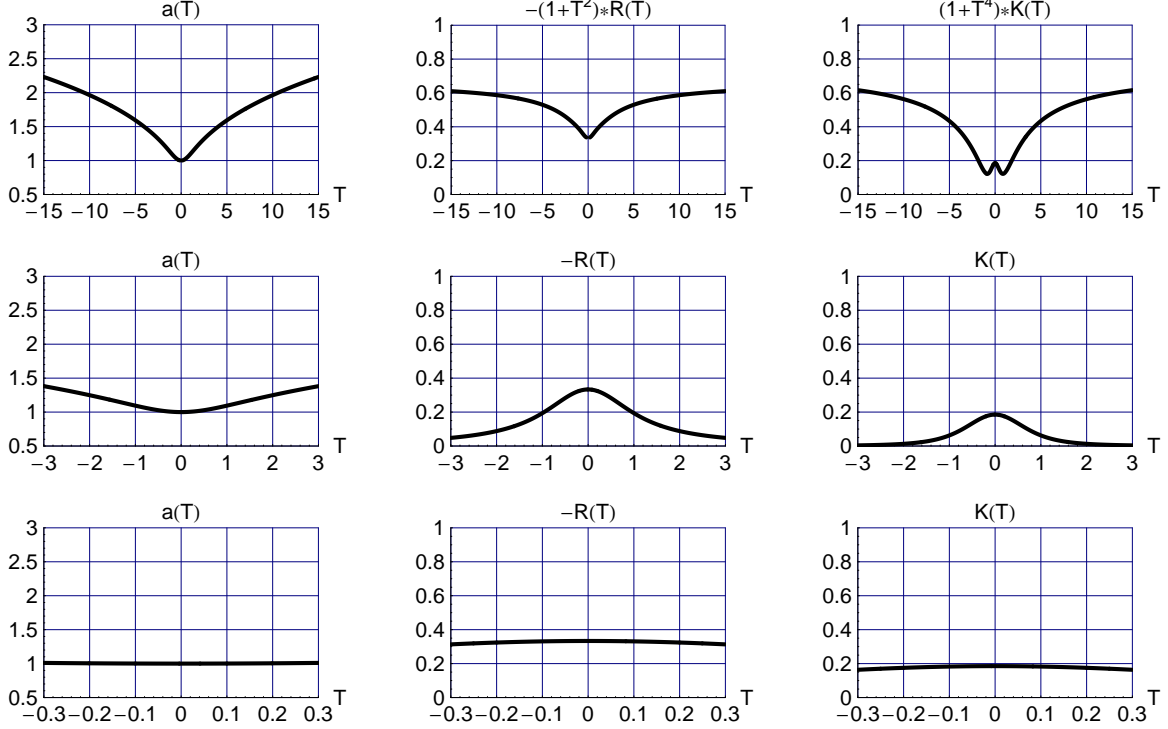


FIG. 4. Ricci curvature scalar  $R(T)$  and Kretschmann curvature scalar  $K(T)$  for the solution  $a(T)$  of Fig. 2. The scaling of  $-R(T)$  and  $K(T)$  in the top-row panels is the same as used in Fig. 3.

In closing, we remark that we have focussed on the dynamics of a time-symmetric nonsingular bounce, with equal equation-of-state parameter  $w_M$  in the pre-bounce phase and the post-bounce phase. But the metric (3.1a) is perfectly suited for the case of a nonsingular bounce with different values of  $w_M$  before and after the bounce. Such a time-asymmetric nonsingular bounce may be preferable for cosmological applications; see Ref. [6] and references therein. The origin of the time-asymmetry may be due to a fundamental arrow-of-time [5] but may also be due to dissipative processes [6], or a combination of both.

## ACKNOWLEDGMENTS

It is a pleasure to thank J.M. Queiruga and Z.L. Wang for comments on the manuscript.

## Appendix A: Bounce solution from initial conditions

The nonsingular bounce solution in Sec. IV was obtained from boundary conditions at the moment of the bounce,  $T = T_B$ . Specifically, the boundary conditions of Figs. 1–4 were given at  $T = T_B = 0$ :  $a(0) \equiv a_B = 1$  and  $\rho_M(0) = r_0$  for values  $r_0 = 1/3$  or  $r_0 = 1/6$ . In this appendix, we present a nonsingular bounce solution obtained from initial boundary conditions, where the actual value of  $T_B$  follows from the solution itself.

Consider the ODEs (3.2a) and (3.2c) for a constant equation-of-state parameter  $w_M$  from (3.3) and set

$$a_B = 1. \quad (\text{A1})$$

Next, choose an arbitrary time

$$T_{\text{start}} \in \mathbb{R}, \quad (\text{A2})$$

at which the initial conditions are the following:

$$a(T_{\text{start}}) = a_{\text{start}} > a_B > 0, \quad (\text{A3a})$$

$$\rho_M(T_{\text{start}}) = \rho_{M-\text{start}} > 0, \quad (\text{A3b})$$

$$a'(T_{\text{start}}) < 0, \quad (\text{A3c})$$

where the prime stands for differentiation with respect to  $T$ . If, for a given value of  $a_{\text{start}}$ , the value of  $\rho_{M-\text{start}}$  is chosen as

$$\rho_{M-\text{start}} = r_0 \left( a_B / a_{\text{start}} \right)^{3[1+w_M]}, \quad (\text{A4})$$

then, for  $r_0 = 1/3$  and  $w_M = 1$ , the bounce dynamics of Figs. 1 and 3 is reproduced, but with  $T_B = 0$  shifted to a possibly nonzero value  $T_B > T_{\text{start}}$ . Similarly, for  $r_0 = 1/6$  and  $w_M = 1$ , the bounce dynamics of Figs. 2 and 4 is reproduced.

The solution from initial conditions (A3) and (A4) at  $T_{\text{start}} = -10$  is shown in Fig. 5. The actual value  $a_{\text{start}} = 2.48312$ , for given values  $r_0 = 1/3$  and  $w_M = 1$  in (A4), is chosen so that the resulting value for  $T_B$  is close to  $T_{\text{start}} + 15$ , which makes the curves of Fig. 5 resemble those of Fig. 1 (with more appropriate digits in the numerical value of  $a_{\text{start}}$ , the curves of Fig. 5 become identical to those of Fig. 1). Different values of  $a_{\text{start}}$ , for the same values of  $T_{\text{start}}$ ,  $r_0$ , and  $w_M$ , give different values for  $T_B$ .

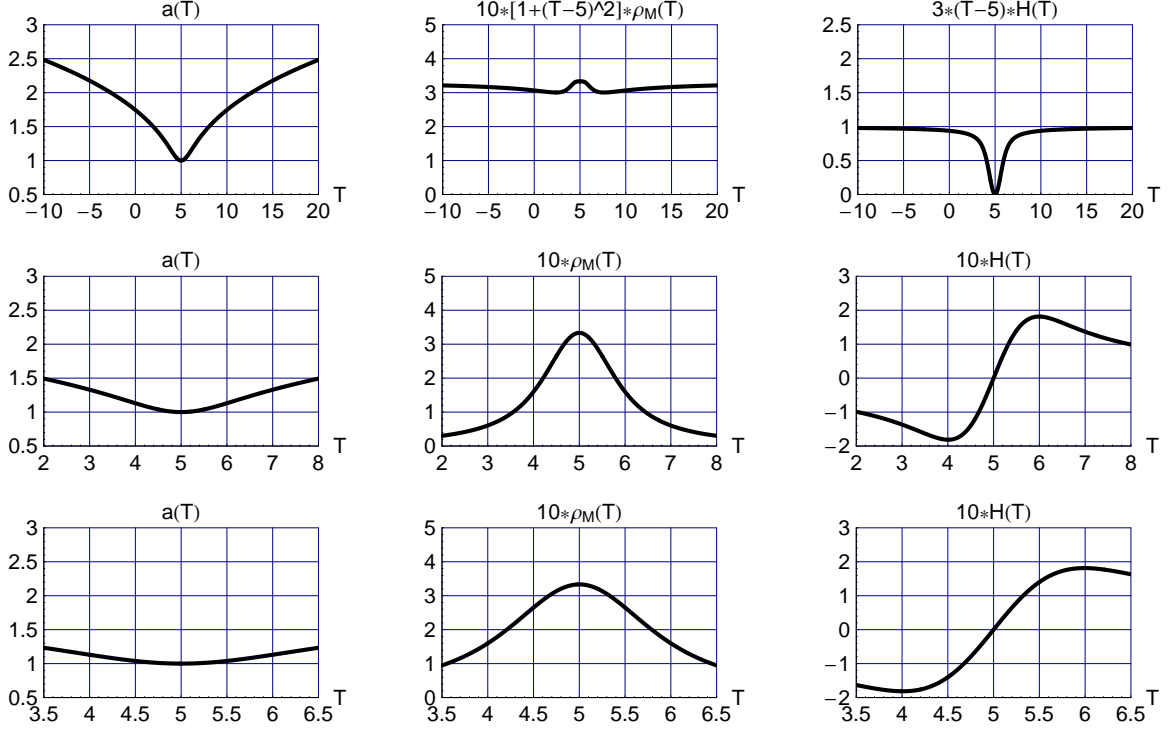


FIG. 5. Solution of the ODEs (3.2a) and (3.2c) for  $a_B = 1$  and constant equation-of-state parameter  $w_M$  from (3.3). The model parameters are  $b = 1$  and  $w_M = 1$ . Different from Fig. 1, there are now initial boundary conditions at  $T = T_{\text{start}} = -10$ . Specifically, the boundary conditions are  $a(-10) = 2.48312$  and  $\rho_M(-10)$  from (A4) for  $r_0 = 1/3$  and  $w_M = 1$ . The numerical solution gives  $T_B \approx 5.000$ . In fact, the numerical pre-bounce solution is obtained over  $T \in [-10, 5 - \Delta T]$ , the analytic solution over  $T \in [5 - \Delta T, 5 + \Delta T]$ , and the numerical post-bounce solution over  $T \in [5 + \Delta T, 20]$ , with  $\Delta T = 1/2$ . The analytic solution for  $a(T)$  is given by (4.2) with  $(T)^{2n}$  on the right-hand side replaced by  $(T - 5)^{2n}$  and coefficients (4.4) for  $N = 4$ , while the analytic solution for  $\rho_M(T)$  follows from (4.1). The numerical post-bounce solution has boundary conditions  $a(5 + \Delta T) = a(5 - \Delta T)$ ,  $\rho_M(5 + \Delta T) = \rho_M(5 - \Delta T)$ , and  $a'(5 + \Delta T) > 0$ . Shown, on the top row, are the dynamic functions  $a(T)$  and  $\rho_M(T)$ , together with the corresponding Hubble parameter  $H(T) \equiv [da(T)/dT]/a(T)$ . The middle and bottom rows zoom in on the bounce at  $T = T_B \approx 5.000$ . In the middle panel of the top row,  $10\rho_M(T)$  is scaled by a further factor  $[1 + (T - 5)^2]$ , in order to display the asymptotic behavior  $\rho_M(T) \propto 1/(T - 5)^2$ . Similarly, in the right panel of the top row,  $H(T)$  is scaled by a factor  $3(T - 5)$ , in order to display the asymptotic behavior  $H(T) \sim (1/3)(T - 5)^{-1}$ .

- 
- [1] A.A. Friedmann, “Über die Krümmung des Raumes” (On the curvature of space), Z. Phys. **10**, 377 (1922); “Über die Möglichkeit einer Welt mit konstanter negativer Krümmung des Raumes” (On the possibility of a world with constant negative curvature), Z. Phys. **21**, 326 (1924).
- [2] S. Weinberg, *Gravitation and Cosmology : Principles and Applications of the General Theory of Relativity* (John Wiley and Sons, New York, 1972).
- [3] F.R. Klinkhamer, “Regularized big bang singularity,” Phys. Rev. D **100**, 023536 (2019), arXiv:1903.10450.
- [4] F.R. Klinkhamer and Z.L. Wang, “Nonsingular bouncing cosmology from general relativity,” arXiv:1904.09961.
- [5] F.R. Klinkhamer and Z.L. Wang, “Asymmetric nonsingular bounce from a dynamic scalar field,” arXiv:1906.04708.
- [6] A. Ijjas and P.J. Steinhardt, “Bouncing cosmology made simple,” Class. Quant. Grav. **35**, 135004 (2018), arXiv:1803.01961.
- [7] F.R. Klinkhamer, “On a soliton-type spacetime defect,” to appear in J. Phys. Conf. Ser., arXiv:1811.01078.
- [8] F.R. Klinkhamer and F. Sorba, “Comparison of spacetime defects which are homeomorphic but not diffeomorphic,” J. Math. Phys. (N.Y.) **55**, 112503 (2014), arXiv:1404.2901.